# Inorganic Chemistry

## Article

# Volatile Magnesium Octahydrotriborate Complexes as Potential CVD Precursors to MgB$_2$. Synthesis and Characterization of Mg(B$_3$H$_8$)$_2$ and Its Etherates

**Do Young Kim,[†] Yu Yang,[‡] John R. Abelson,[‡] and Gregory S. Girolami*,[†]**

*School of Chemical Sciences and Department of Materials Science and Engineering, University of Illinois at Urbana−Champaign, 600 South Mathews Avenue, Urbana, Illinois 61801*

The solid-state reaction of MgBr$_2$ and NaB$_3$H$_8$ at 20 °C, followed by sublimation at 80 °C and 0.05 Torr, affords Mg(B$_3$H$_8$)$_2$ as a white solid. Similar reactions with MgBr$_2$(Et$_2$O) and MgBr$_2$(Me$_2$O)$_{1.5}$ afford the crystalline ether adducts Mg(B$_3$H$_8$)$_2$(Et$_2$O)$_2$ and Mg(B$_3$H$_8$)$_2$(Me$_2$O)$_2$, respectively. In contrast, reactions of MgBr$_2$ with NaB$_3$H$_8$, the presence of excess solvent result in the formation of nonvolatile, probably ionic, magnesium compounds of the type [MgL$_x$][B$_3$H$_8$]$_2$. The adducts Mg(B$_3$H$_8$)$_2$(Et$_2$O)$_2$ and Mg(B$_3$H$_8$)$_2$(Me$_2$O)$_2$ are the first crystallographically characterized magnesium complexes of the B$_3$H$_8^-$ ligand; in both structures, the magnesium center adopts a distorted cis-octahedral geometry with two bidentate B$_3$H$_8$ groups and two Et$_2$O ligands. Owing to their volatility, Mg(B$_3$H$_8$)$_2$-(Et$_2$O)$_2$ and Mg(B$_3$H$_8$)$_2$(Me$_2$O)$_2$ are potential precursors for the deposition of MgB$_2$ thin films, although preliminary efforts to employ them as chemical vapor deposition sources produce boron-rich MgB$_x$ films instead, with $x \approx 7$. Finally, the synthesis and structure of Cp$_2$Mg(thf) are described: this mono-thf adduct of Cp$_2$Mg bears two $\eta^5$-Cp groups, unlike other Lewis base adducts of Cp$_2$Mg, which contain one $\eta^5$-Cp group and one $\eta^1$- or $\eta^2$-Cp group.

## Introduction

Magnesium diboride (MgB$_2$) has been the subject of considerable interest since the discovery in 2001 that it becomes superconducting at 39 K.[1] MgB$_2$ has highly attractive properties for applications in superconducting electronics: in addition to having the highest critical temperature of all intermetallic superconductors, it has a long coherence length of ca. 5 nm and a high-energy gap.[2−4] These properties suggest that MgB$_2$-based superconducting circuits should operate more rapidly, and at a higher temperature, than circuits based on niobium alloys.

Because multilayer tunneling junctions are core elements in integrated circuits, intensive research has been directed toward the development of methods to grow high-quality MgB$_2$ thin films. Successful depositions of such films have been achieved by co-evaporation of Mg and B in extremely clean environments,[5] by boron deposition followed by ex-situ annealing with Mg vapor in a sealed tube[6] and by a hybrid physical−chemical vapor deposition (HPCVD) technique in which B$_2$H$_6$ reacts with Mg vapor.[7] Methodological improvements are still required, however, to achieve the large-scale fabrication of multilayer MgB$_2$ tunneling junctions, which require the deposition of stoichiometric, crystalline films via an in-situ process at a low temperature. No purely chemical vapor deposition (CVD) route to MgB$_2$ films has been described. One obstacle is that magnesium tends to evaporate from the growth surface at temperatures above 425 °C,[8] leaving behind boron or boron-rich films.

---

* To whom correspondence should be addressed. E-mail: girolami@scs.uiuc.edu.

† Department of Chemistry.

‡ Department of Materials Science and Engineering.

(1) Nagamatsu, J.; Nakagawa, N.; Muranaka, T.; Zenitani, Y.; Akimitsu, J. *Nature* **2001**, *410*, 63−64.

(2) Xu, M.; Kitazawa, H.; Takano, Y.; Ye, J.; Nishida, K.; Abe, H.; Matsushita, A.; Tsujii, N.; Kido, G. *Appl. Phys. Lett.* **2001**, *79*, 2779−2781.

(3) Schmidt, H.; Zasadzinski, J. F.; Gray, K. E.; Hinks, D. G. *Phys. Rev. Lett.* **2002**, *88*, 127001/1−127001/4.

(4) Tsuda, S.; Yokoya, T.; Kiss, T.; Takano, Y.; Togano, K.; Kito, H.; Ihara, H.; Shin, S. *Phys. Rev. Lett.* **2001**, *87*, 177006/1−177006/4.

(5) Ueda, K.; Naito, M. *J. Appl. Phys.* **2003**, *93*, 2113−2120.

(6) Kang, W. N.; Kim, H. J.; Choi, E. M.; Jung, C. U.; Lee, S. L. *Science* **2001**, *292*, 1521−1523.

(7) Zeng, X. H.; Pogrebnyakov, A. V.; Kotcharov, A.; Jones, J. E.; Xi, X. X.; Lysczek, E. M.; Redwing, J. M.; Xu, S. Y.; Lettieri, J.; Schlom, D. G.; Tian, W.; Pan, X. Q.; Liu, Z. K. *Nat. Mater.* **2002**, *1*, 35−38.

Another obstacle to preparing $MgB_2$ by CVD is that few magnesium compounds are volatile and, of those, none has been shown to be chemically suited as a precursor for this phase. Several magnesium complexes of tetrahydroborate ($BH_4^-$), octahydrotriborate ($B_3H_8^-$), and nonahydrohexaborate ($B_6H_9^-$) groups have been described. Specifically, the binary complex $Mg(BH_4)_2$ is known,[9] as are several Lewis base adducts, $Mg(BH_4)_2L_x$ (L = ethers, amines, or sulfoxides).[10−14] For the higher boron hydrides, ionic species of the form $[Mg(L)_6][B_3H_8]_2$, where L is $NH_3$, thf, or $^1/_3$-diglyme, can be prepared by reaction of $Mg(BH_4)_2L_x$ with diborane,[15−17] and $Mg(B_6H_9)_2(thf)_2$ can be prepared by reaction of $MgMe_2$ or $MeMgBr$ with $B_6H_{10}$ in thf.[18]

We now describe the synthesis of bis(octahydrotriborate)-magnesium $Mg(B_3H_8)_2$ and its Lewis base adducts, $Mg(B_3H_8)_2(Et_2O)_2$ and $Mg(B_3H_8)_2(Me_2O)_2$. These molecules are volatile and are the first crystallographically characterized magnesium complexes of the $B_3H_8$ ligand. Owing to their volatility, $Mg(B_3H_8)_2(Et_2O)_2$ and $Mg(B_3H_8)_2(Me_2O)_2$ are potential precursors for the deposition of $MgB_2$ thin films, and we describe preliminary efforts to grow thin films from them under CVD conditions. These new compounds closely resemble other volatile $MB_xH_y$ precursors that are known to afford high-quality films of transition metal diboride materials such as $TiB_2$, $CrB_2$, $ZrB_2$, and $HfB_2$.[19−23]

## Results and Discussion

**Synthesis and Characterization of $Mg(B_3H_8)_2$.** Our initial efforts to carry out the reaction of $MgBr_2$ and $NaB_3H_8$ in ether solvents, such as tetrahydrofuran or 1,2-dimethoxyethane, afforded insoluble and nonvolatile reaction products. This result is consistent with two previous studies, which showed that magnesium $B_3H_8$ compounds convert to ionic products in the presence of coordinating ether solvents. For example, the reactions of $Mg(BH_4)_2$ with $B_2H_6$ in tetrahy-
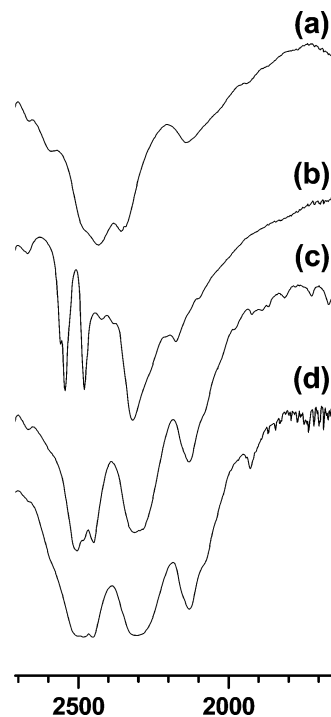
**Figure 1.** B−H stretching region in the infrared spectra of (a) $NaB_3H_8$, (b) $Mg(B_3H_8)_2$, (c) $Mg(B_3H_8)_2(Et_2O)_2$, and (d) $Mg(B_3H_8)_2(Me_2O)_2$.

drofuran or bis(2-methoxyethyl)ether (diglyme) afford the salts $[Mg(thf)_6][B_3H_8]_2$[15] and $[Mg(diglyme)_2][B_3H_8]_2$,[16] in which the magnesium dications are exclusively coordinated to ether molecules. The ionic nature of these latter materials is shown by the absence of Mg−H−B stretching bands near $2300$ cm$^{-1}$ in their IR spectra. Similarly, Lewis base adducts of $Mg(BH_4)_2$ have different structures depending on the stoichiometry: the 3:1 complexes $Mg(BH_4)_2L_3$ (L = thf, *tert*-butylamine, or piperdine) and the 4:1 complex $Mg(BH_4)_2$-$(pyridine)_4$ are molecular species, but the 6:1 adducts $[MgL_6][BH_4]_2$ (L = benzylamine or dimethyl sulfoxide) are ionic salts.[11,13] Attempts to carry out the reaction of $MgBr_2$ and $NaB_3H_8$ in diethyl ether also did not lead to the formation of a soluble magnesium $B_3H_8$ product, evidently because no reaction takes place.
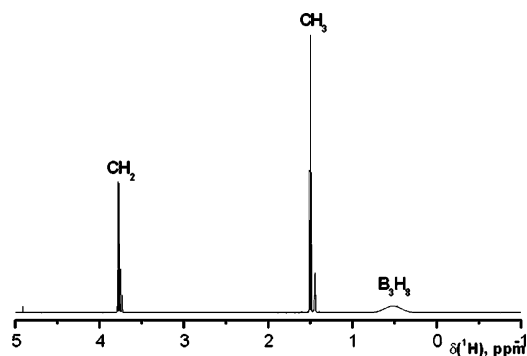
A key to the synthesis of volatile magnesium $B_3H_8$ complexes is the use of solvent-free reaction methods. Thus, mixing powders of $MgBr_2$ and $NaB_3H_8$ at 20 °C, followed by heating to 80 °C in a vacuum (0.05 Torr) results in the formation of a new compound $Mg(B_3H_8)_2$ (**1**), which can be isolated as a white solid by condensation on a cold finger. Attempts to obtain single crystals of **1** suitable for X-ray diffraction have been unsuccessful.

The infrared spectrum of **1** (Figure 1) contains two terminal B−H stretches at 2543 and 2479 cm$^{-1}$, one bridging Mg−H−B stretch at 2316 cm$^{-1}$ and a bridging B−H−B stretch at 2175 cm$^{-1}$. All of these bands are consistent with the presence of coordinated $B_3H_8$ groups. The B−H stretching bands for **1** are similar to those observed for transition metal octahydrotriborate complexes[20,24−26] with two excep-

(8) Fan, Z. Y.; Hinks, D. G.; Newman, N.; Rowell, J. M. *Appl. Phys. Lett.* **2001**, *79*, 87−89.
(9) Černý, R.; Filinchuk, Y.; Hagemann, H.; Yvon, K. *Angew. Chem.* **2007**, *46*, 5765−5767.
(10) Soloveichik, G. L.; Andrus, M.; Lobkovsky, E. B. *Inorg. Chem.* **2007**, *46*, 3790−3791.
(11) Bremer, M.; Noth, H.; Warchhold, M. *Eur. J. Inorg. Chem.* **2003**, 111−119.
(12) Lobkovskii, E. B.; Titov, L. V.; Psikha, S. B.; Antipin, M. Y.; Struchkov, Y. T. *J. Struct. Chem.* **1982**, *23*, 644−646.
(13) Noeth, H. *Z. Naturforsch. B* **1982**, *37*, 1499−1503.
(14) Lobkovskii, É. B.; Titov, L. V.; Levicheva, M. D.; Chekhlov, A. N. *J. Struct. Chem.* **1990**, *31*, 506−508.
(15) Hermanek, S.; Plesek, J. *Collect. Czech. Chem. Commun.* **1966**, *31*, 177−89.
(16) Titov, L. V.; Levicheva, M. D.; Psikha, S. B. *Zh. Neorg. Khim.* **1984**, *29*, 668−73; *Russ. J. Inorg. Chem.* **1984**, *29*, 386−389.
(17) Levicheva, M. D.; Titov, L. V.; Psikha, S. B. *Zh. Neorg. Khim.* **1987**, *32*, 510−12; *Russ. J. Inorg. Chem.* **1987**, *32*, 284−285.
(18) Denton, D. L.; Clayton, W. R.; Mangion, M.; Shore, S. G.; Meyers, E. A. *Inorg. Chem.* **1976**, *15*, 541−548.
(19) Jensen, J. A.; Gozum, J. E.; Pollina, D. M.; Girolami, G. S. *J. Am. Chem. Soc.* **1988**, *110*, 1643−1644.
(20) Goedde, D. M.; Girolami, G. S. *J. Am. Chem. Soc.* **2004**, *126*, 12230−12231.
(21) Jayaraman, S.; Klein, E. J.; Yang, Y.; Kim, D. Y.; Girolami, G. S.; Abelson, J. R. *J. Vac. Sci. Technol., A* **2005**, *23*, 631−633.
(22) Sung, J.; Goedde, D. M.; Girolami, G. S.; Abelson, J. R. *J. Appl. Phys.* **2002**, *91*, 3904−3911.
(23) Jayaraman, S.; Yang, Y.; Kim, D. Y.; Girolami, G. S.; Abelson, J. R. *J. Vac. Sci. Technol., A* **2005**, *23*, 1619−1625.

(24) Gaines, D. F.; Morris, J. H. *J. Chem. Soc., Chem. Commun.* **1975**, 626−7.
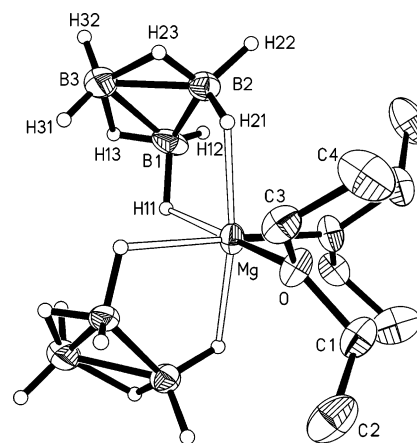(25) Lippard, S. J.; Ucko, D. *Inorg. Chem.* **1968**, *7*, 1051−1056.

**Figure 2.** ^{1}H NMR spectrum of Mg(B$_3$H$_8$)$_2$(Et$_2$O)$_2$ (**2**) in (C$_2$D$_5$)$_2$O at 20 °C.



**Figure 3.** Molecular structure of **2**. Ellipsoids are drawn at the 35% probability level, except for hydrogen atoms, which are represented as arbitrarily sized spheres. Methyl and methylene hydrogen atoms have been deleted for clarity.



**Figure 4.** Molecular structure of Mg(B$_3$H$_8$)$_2$(Me$_2$O)$_2$ (**3**). Ellipsoids are drawn at the 35% probability level, except for hydrogen atoms, which are represented as arbitrarily sized spheres. Methyl hydrogen atoms have been deleted for clarity.

tions. First, the 2316 cm$^{-1}$ frequency for the M—H—B stretching band is higher than those of 2000–2200 cm$^{-1}$ seen for transition metal B$_3$H$_8$ complexes.[25,26] The higher frequency seen in **1** reflects the lower mass of the magnesium atom and the less-covalent character of the Mg—B$_3$H$_8$ interaction. Second, the 2316 cm$^{-1}$ band is more intense than the M—H—B stretching bands seen for transition metal complexes. Further characterization of **1** (for example, by solution NMR spectroscopy) has been precluded by the insolubility of **1** in common organic solvents, including pentane, benzene, toluene, dichloromethane, tetrahydrofuran, and dioxane. Protic solvent such as ethanol and water react with **1**, with vigorous evolution of gas.

**Synthesis and Characterization of Mg(B$_3$H$_8$)$_2$(Et$_2$O)$_2$ and Mg(B$_3$H$_8$)$_2$(Me$_2$O)$_2$.** Mixing powders of the etherate MgBr$_2$(Et$_2$O) and NaB$_3$H$_8$ at 20 °C, followed by heating to 70 °C and 0.05 Torr, yields a colorless crystalline sublimate of stoichiometry Mg(B$_3$H$_8$)$_2$(Et$_2$O)$_2$ (**2**). A similar reaction with MgBr$_2$(Me$_2$O)$_{1.5}$ affords the dimethyl ether analogue Mg(B$_3$H$_8$)$_2$(Me$_2$O)$_2$ (**3**). The IR spectrum of **2** features strong bands at 2506 and 2448 cm$^{-1}$ due to terminal B—H stretches, a strong broad band at 2302 cm$^{-1}$ for the Mg—H—B stretch, and a medium-intensity band at 2129 cm$^{-1}$ due to the B—H—B stretches (Figure 1). The IR spectrum of **3** in the B—H stretching region is very similar to that of **2**.

Like **1**, compounds **2** and **3** react with protic solvents and are insoluble in almost all nonprotic solvents; we attribute the insolubility in strongly coordinating ethers such as tetrahydrofuran or 1,2-dimethoxyethane to the formation of ionic salts (see above). Compound **2** is, however, soluble in diethyl ether. The weaker Lewis basicity of Et$_2$O is probably responsible for its ability to dissolve Mg(B$_3$H$_8$)$_2$(Et$_2$O)$_2$ without forming insoluble ionic salts.

The ^{1}H NMR spectrum of **2** in (C$_2$D$_5$)$_2$O at 20 °C (Figure 2) shows a broad, unresolved signal at δ 0.52 for the B$_3$H$_8$ groups and characteristic resonances for the Et$_2$O protons. The ^{11}B NMR spectrum at 20 °C contains a broad, unresolved resonance at δ −31.7. Similar ^{1}H and ^{11}B NMR spectra are seen at −80 °C, which suggests that the B$_3$H$_8$ ligand is fluxional on the NMR time scale even at this temperature. The mass spectrum of **2** contains no parent peak (m/z = 205); instead, the most intense peak in the spectrum (m/z = 318)
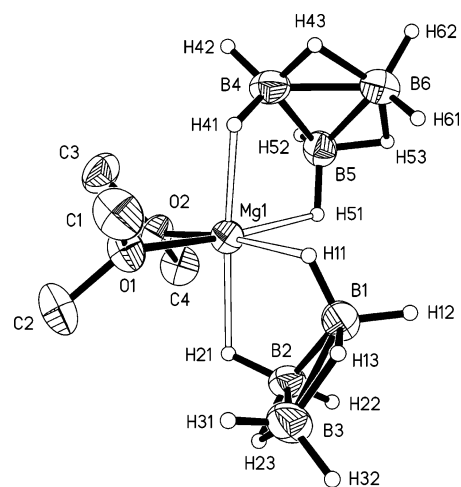
corresponds to Mg$_2$(B$_3$H$_8$)$_3$(Et$_2$O)$_2$$^+$. The mass spectrum of **3** is similar, the most intense signal (at m/z = 262) being due to Mg$_2$(B$_3$H$_8$)$_3$(Me$_2$O)$_2$$^+$.

The molecular structures of **2** and **3** are shown in Figures 3 and 4; crystallographic data, and selected bond distances and angles are listed in Tables 1–3. The magnesium center in the diethyl ether adduct **2** adopts a distorted cis-octahedral geometry with two bidentate B$_3$H$_8$ groups and two Et$_2$O ligands. The Mg—H distances are identical within experimental error at 1.99(3) and 2.01(4) Å, and the Mg⋯B distances are nearly identical at 2.575(5) and 2.591(5) Å. The B—H distances of 1.17(2) Å within the Mg—H—B units are slightly longer than the terminal B—H distances of 1.12-(3) Å, as expected. As seen in other metal complexes of the bidentate B$_3$H$_8$$^-$ ligand,[20,27–30] the B—B distance for the

(26) Gaines, D. F.; Hildebrandt, S. J. *Inorg. Chem.* **1978**, *17*, 794–806.

(27) Beckett, M. A.; Brassington, D. S.; Coles, S. J.; Gelbrich, T.; Hursthouse, M. B. *Polyhedron* **2003**, *22*, 1627–1632.
(28) Grebenik, P. D.; Leach, J. B.; Green, M. L. H.; Walker, N. M. *J. Organomet. Chem.* **1988**, *345*, C31–C34.
(29) Calabrese, J. C.; Gaines, D. F.; Hildebrandt, S. J.; Morris, J. H. *J. Am. Chem. Soc.* **1976**, *98*, 5489–5492.
(30) Guggenberger, L. J. *Inorg. Chem.* **1970**, *9*, 367–373.

**Table 1.** Crystallographic Data for **2**, **3**, and **4**

| | **2** | **3** | **4** |
|---|---|---|---|
| formula | $MgB_6C_8H_{36}O_2$ | $MgB_6C_4H_{28}O_2$ | $MgC_{14}H_{18}O$ |
| fw | 253.54 | 197.43 | 226.59 |
| $T$, °C | −80 | −80 | −80 |
| space group | $P2_12_12$ | $Pca2_1$ | $C2/c$ |
| $a$, Å | 7.337(4) | 13.9644(19) | 12.414(16) |
| $b$, Å | 15.586(8) | 6.9088(10) | 9.855(12) |
| $c$, Å | 8.332(4) | 16.034(2) | 11.556(14) |
| $\beta$, deg | 90 | 90 | 116.72(2) |
| $V$, Å$^3$ | 952.7(9) | 1546.9(4) | 1263(3) |
| $Z$ | 2 | 4 | 4 |
| $\rho_{calcd}$, g cm$^{-3}$ | 0.884 | 0.848 | 1.192 |
| $\lambda$, Å | 0.71073 | 0.71073 | 0.71073 |
| $\mu_{calcd}$, cm$^{-1}$ | 0.81 | 0.86 | 1.17 |
| transmission coeff | 0.956−0.966 | 0.954−0.991 | 0.972−0.995 |
| unique reflns | 1750 | 2837 | 1161 |
| params | 151 | 186 | 101 |
| R1$^a$ | 0.0726 | 0.0347 | 0.0824 |
| wR2$^b$ | 0.1579 | 0.0796 | 0.2045 |

$^a$ R1 $= \sum||F_o| - |F_c||/\sum|F_o|$ for reflections with $F_o^2 > 2\sigma(F_o^2)$. $^b$ wR2 $= [\sum w(F_o^2 - F_c^2)^2/\sum w(F_o^2)^2]^{1/2}$ for all reflections.

nonbridged B−B bond is the shortest at 1.779(7) Å, whereas the B−B distances for the two hydrogen bridged B−B bonds are slightly longer at 1.795(7) and 1.809(7) Å.

The Mg−H distances of 1.99(3) and 2.01(4) Å in **2** lie in the range 1.97−2.24 Å seen in magnesium complexes of the BH$_4$ ligand.[9−14,31,32] The Mg···B distances of 2.575(5) and 2.591(5) Å in **2** are slightly longer than those of 2.40−2.54 Å found in magnesium complexes of bidentate BH$_4$ ligands[11−14] but are much longer than those of 2.21−2.29 Å seen in magnesium complexes containing tridentate BH$_4$ ligands,[10,31,32] as expected.

The molecular geometry of the dimethyl ether adduct **3** is very similar to that of **2**: the magnesium center is six-coordinate with two bidentate B$_3$H$_8^-$ ligands and two mutually cis dimethyl ether groups. All Mg−H and Mg···B distances in **3** are also nearly identical to those in **2**: the average Mg−H distance is 1.96(4) Å, and the average Mg···B distance is 2.565(6) Å. The dimethyl ether ligand in **3** should be sterically less demanding than the diethyl ether ligand in **2**, and this difference may be responsible for a subtle difference in the relative orientations adopted by the coordinated B$_3$H$_8$ groups. If we focus on the "unbound" BH$_2$ group within each B$_3$H$_8$ ligand, in **3** one is proximal to the dimethyl ether group and the other is distal, whereas in **2** both "unbound" BH$_2$ groups are distal to the diethyl ether ligands.

Most likely, the ether groups in **2** and **3** occupy mutually cis positions so as to minimize interligand steric repulsions. Interestingly, the molecular structures of **2** and **3** differ from that of the chromium analogue Cr(B$_3$H$_8$)$_2$(Et$_2$O)$_2$,[20] which adopts a trans-octahedral geometry. Electronic factors relating to the Jahn−Teller effect dominate in determining the structure of the d$^4$ chromium complex: the diethyl ether ligands, which generate the weakest ligand field splitting, are relegated to the axial positions so as to maximize the

ligand field stabilization energy. In contrast, no such electronic factors operate in Mg(B$_3$H$_8$)$_2$(Et$_2$O)$_2$.

**Attempts to Grow MgB$_2$ Thin Films.** Compound **1** is not an ideal precursor for CVD because it sublimes very slowly and with some decomposition; the ether adducts **2** and **3** sublime much more readily, and so we investigated the deposition of films from these compounds. For **2**, the onset temperature for film growth is 400 °C. The resulting deposit exhibits a B/Mg ratio of ∼7 (82 at. % boron and 12 at. % magnesium) as determined by Auger electron spectroscopy. For **3**, the onset temperature is 450 °C, and the films deposited under these conditions consist of 70 at. % boron, 20 at. % carbon, 8 at. % oxygen, and essentially no magnesium. For both compounds, the onset temperature is evidently high enough that sublimation of magnesium competes with film growth, so that the resulting films are boron-rich.[39] Further characterization of these non-stoichiometric films was not pursued.

The solid-state decomposition of [Mg(diglyme)$_2$][B$_3$H$_8$]$_2$ at 185 °C yields Mg(BH$_4$)$_2$, MgB$_{12}$H$_{12}$, H$_2$, and B$_5$H$_9$.[16] The solid-state decomposition of [Mg(NH$_3$)$_6$][B$_3$H$_8$]$_2$ at 120−140 °C is reported to proceed somewhat differently, affording Mg(BH$_4$)$_2$(NH$_3$)$_2$, B$_3$N$_3$H$_6$, (BNH)$_n$, and H$_2$.[17] These findings suggest that the thermolysis mechanism depends on the identity of the Lewis base; thus, magnesium octahydrotriborate complexes with other neutral ligands may be more successful in affording MgB$_2$ by CVD (or plasma-assisted CVD) methods.

**Synthesis and Characterization of Cp$_2$Mg(thf).** Attempts to prepare a Cp-containing magnesium compound of the B$_3$H$_8$ ligand by treating [CpMgCl(Et$_2$O)]$_2$ with NaB$_3$H$_8$ in pentane/tetrahydrofuran resulted instead in the isolation of the B$_3$H$_8$-free product Cp$_2$Mg(thf) (**4**). The structure of the bis-thf adduct Cp$_2$Mg(thf)$_2$ has been studied,[33] but the structure of the mono-thf adduct has not been previously determined.

The molecular structure of **4** is shown in Figure 5; crystallographic data, and selected bond distances and angles are listed in Tables 1 and 4. The magnesium center is coordinated to two $\eta^5$-Cp groups and one thf group. The Mg−C distances lie in the narrow range of 2.441(6)−2.482(6) Å and average 2.460(14) Å. The Mg−O distance is 2.093(6) Å. The two Cp-ring planes describe a dihedral angle of 41.3°. Few adducts of bis(cyclopentadienyl)magnesium have been crystallographically characterized: among these are Cp$_2$Mg(thf)$_2$,[33] Cp$_2$Mg(NH$_2$CH(i-Pr)$_2$),[34] and Cp$_2$Mg-(NH$_2$-t-Bu)(thf).[35] One difference in the structure of **4** is that both Cp groups adopt $\eta^5$ coordination modes; in contrast, Cp$_2$Mg(thf)$_2$ and Cp$_2$Mg(NH$_2$-$t$-Bu)(thf) each contain one $\eta^5$- and one $\eta^1$-Cp group, and Cp$_2$Mg(NH$_2$CH($i$-Pr)$_2$) contains $\eta^5$- and $\eta^2$-Cp groups. The larger steric congestion in these

(31) Bremer, M.; Linti, G.; Noth, H.; Thomann-Albach, M.; Wagner, G. Z. *Anorg. Allg. Chem.* **2005**, *631*, 683−697.

(32) Prust, J.; Most, K.; Muller, I.; Alexopoulos, E.; Stasch, A.; Uson, I.; Roesky, H. W. *Z. Anorg. Allg. Chem.* **2001**, *627*, 2032−2037.

(33) Jaenschke, A.; Paap, J.; Behrens, U. *Organometallics* **2003**, *22*, 1167−1169.

(34) Xia, A. B.; Heeg, M. J.; Winter, C. H. *J. Am. Chem. Soc.* **2002**, *124*, 11264−11265.

(35) Olmstead, M. M.; Grigsby, W. J.; Chacon, D. R.; Hascall, T.; Power, P. P. *Inorg. Chim. Acta* **1996**, *251*, 273−284.

**Figure 5.** Molecular structure of Cp₂Mg(thf) (**4**). Ellipsoids are drawn at the 35% probability level except for hydrogen atoms, which are represented as arbitrarily sized spheres.

**Table 2.** Selected Bond Lengths (Å) and Angles (deg) for **2**[a]

| Bond Lengths (Å) | | | |
|---|---|---|---|
| Mg−O | 2.025(3) | B(1)−H(12) | 1.12(3) |
| Mg−B(1) | 2.575(5) | B(1)−H(13) | 1.02(4) |
| Mg−B(2) | 2.591(5) | B(2)−H(21) | 1.17(2) |
| Mg−H(11) | 1.99(3) | B(2)−H(22) | 1.11(3) |
| Mg−H(21) | 2.01(4) | B(2)−H(23) | 1.02(4) |
| B(1)−B(2) | 1.779(7) | B(3)−H(13) | 1.43(4) |
| B(1)−B(3) | 1.795(10) | B(3)−H(23) | 1.43(4) |
| B(2)−B(3) | 1.809(7) | B(3)−H(31) | 1.02(3) |
| B(1)−H(11) | 1.17(2) | B(3)−H(32) | 1.02(3) |
| Bond Angles (deg) | | | |
| O′−Mg−O | 93.66(16) | H(11)−Mg−H(21) | 90.0(15) |
| O′−Mg−H(11) | 92.9(8) | B(1)−B(2)−B(3) | 60.0(3) |
| O−Mg−H(11) | 172.8(9) | B(1)−B(3)−B(2) | 59.2(3) |
| O′−Mg−H(21) | 100.8(10) | B(2)−B(1)−B(3) | 60.8(3) |
| O−Mg−H(21) | 85.8(8) | | |

[a] Symmetry transformations used to generate equivalent atoms: ′ = −x + 2, −y + 2, z.

latter compounds is probably responsible for the lower hapticity of the second Cp group.

## Experimental Section

All experiments were carried out under vacuum or under argon by using standard Schlenk techniques. Solvents were distilled under nitrogen from sodium/benzophenone immediately before use. NaB₃H₈ was prepared by a literature procedure,[36] and MgBr₂ and MgBr₂(Et₂O) were used as received (Aldrich). Dimethyl ether was purchased from Matheson. Microanalyses were performed by the University of Illinois Microanalytical Laboratory. The IR spectra were recorded on a Nicolet Impact 410 instrument as Nujol mulls between KBr plates. The ¹H and ¹¹B NMR data were collected on Varian Unity Inova 600 instrument at 599.761 and 192.427 MHz, respectively. Chemical shifts are reported in $\delta$ units (positive shifts to high frequency) relative to tetramethylsilane or BF₃·Et₂O. Field ionization (FI) mass spectra were recorded on a Micromass 70-VSE mass spectrometer. The shapes of all peak envelopes correspond with those calculated from the natural abundance isotopic distributions. Melting points were determined in closed capillaries under argon on a Thomas−Hoover Unimelt apparatus. Auger spectra were recorded on a Physical Electronics PHI 660 system with a beam energy of 5 kV and a base pressure of ca. $1 \times 10^{-10}$ Torr.

(36) Goedde, D. M.; Windler, G. K.; Girolami, G. S. *Inorg. Chem.* **2007**, *46*, 2814−2823.

**Table 3.** Selected Bond Lengths (Å) and Angles (deg) for **3**

| Bond Lengths (Å) | | | |
|---|---|---|---|
| Mg(1)−O(2) | 2.0181(15) | B(1)−H(13) | 1.10(2) |
| Mg(1)−O(1) | 2.0279(14) | B(2)−H(21) | 1.167(19) |
| Mg(1)−B(2) | 2.557(3) | B(2)−H(22) | 1.144(19) |
| Mg(1)−B(4) | 2.559(3) | B(2)−H(23) | 1.11(2) |
| Mg(1)−B(1) | 2.570(3) | B(3)−H(13) | 1.38(2) |
| Mg(1)−B(5) | 2.572(3) | B(3)−H(23) | 1.45(2) |
| Mg(1)−H(11) | 1.967(19) | B(3)−H(31) | 1.06(2) |
| Mg(1)−H(21) | 1.973(16) | B(3)−H(32) | 1.06(2) |
| Mg(1)−H(41) | 1.91(2) | B(4)−H(41) | 1.19(2) |
| Mg(1)−H(51) | 1.98(2) | B(4)−H(42) | 1.08(2) |
| B(1)−B(2) | 1.795(4) | B(4)−H(43) | 1.17(3) |
| B(1)−B(3) | 1.802(4) | B(5)−H(51) | 1.14(2) |
| B(2)−B(3) | 1.803(5) | B(5)−H(52) | 1.10(2) |
| B(4)−B(5) | 1.777(4) | B(5)−H(53) | 1.15(2) |
| B(4)−B(6) | 1.804(5) | B(6)−H(43) | 1.45(2) |
| B(5)−B(6) | 1.780(4) | B(6)−H(53) | 1.39(2) |
| B(1)−H(11) | 1.140(19) | B(6)−H(61) | 1.11(2) |
| B(1)−H(12) | 1.13(2) | B(6)−H(62) | 1.17(2) |
| Bond Angles (deg) | | | |
| O(1)−Mg(1)−O(2) | 91.80(6) | H(11)−Mg(1)−H(51) | 89.4(8) |
| O(1)−Mg(1)−H(11) | 90.3(6) | H(21)−Mg(1)−H(41) | 170.3(8) |
| O(1)−Mg(1)−H(21) | 91.9(5) | H(21)−Mg(1)−H(51) | 93.6(8) |
| O(1)−Mg(1)−H(41) | 85.8(7) | H(41)−Mg(1)−H(51) | 88.8(9) |
| O(1)−Mg(1)−H(51) | 174.6(6) | B(2)−B(1)−B(3) | 60.15(18) |
| O(2)−Mg(1)−H(11) | 172.8(6) | B(1)−B(2)−B(3) | 60.14(17) |
| O(2)−Mg(1)−H(21) | 83.2(6) | B(1)−B(3)−B(2) | 59.72(16) |
| O(2)−Mg(1)−H(41) | 106.2(6) | B(5)−B(4)−B(6) | 59.60(17) |
| O(2)−Mg(1)−H(51) | 89.1(5) | B(4)−B(5)−B(6) | 60.97(18) |
| H(11)−Mg(1)−H(21) | 89.9(8) | B(5)−B(6)−B(4) | 59.43(17) |
| H(11)−Mg(1)−H(41) | 80.8(8) | | |

**Table 4.** Selected Bond Lengths (Å) and Angles (deg) for **4**

| Bond Lengths (Å) | | | |
|---|---|---|---|
| Mg(1)−C(1) | 2.451(7) | C(1)−C(5) | 1.427(7) |
| Mg(1)−C(2) | 2.441(6) | C(2)−C(3) | 1.410(7) |
| Mg(1)−C(3) | 2.482(6) | C(3)−C(4) | 1.418(7) |
| Mg(1)−C(4) | 2.460(6) | C(4)−C(5) | 1.413(8) |
| Mg(1)−C(5) | 2.464(6) | C(6)−C(7) | 1.505(8) |
| Mg(1)−O(1) | 2.093(6) | C(6)−O(1) | 1.484(6) |
| C(1)−C(2) | 1.389(7) | | |
| Bond Angles (deg) | | | |
| C(1)−Mg(1)−C(3) | 55.3(2) | C(4)−Mg(1)−C(3) | 33.35(16) |
| C(1)−Mg(1)−C(4) | 55.4(2) | O(1)−Mg(1)−C(1) | 83.01(14) |
| C(1)−Mg(1)−C(5) | 33.76(18) | O(1)−Mg(1)−C(2) | 107.36(15) |
| C(2)−Mg(1)−C(1) | 32.99(18) | O(1)−Mg(1)−C(3) | 137.99(15) |
| C(2)−Mg(1)−C(3) | 33.28(17) | O(1)−Mg(1)−C(4) | 126.58(16) |
| C(2)−Mg(1)−C(4) | 55.08(18) | O(1)−Mg(1)−C(5) | 93.46(15) |
| C(2)−Mg(1)−C(5) | 55.34(19) | | |

**Bis(octahydrotriborato)magnesium, Mg(B₃H₈)₂, (1).** Solid MgBr₂ (2.97 g, 16.1 mmol) and NaB₃H₈ (1.02 g, 16.1 mmol) were ground together briefly in a mortar and pestle. The dry mixture was transferred to a 250 mL round-bottomed flask, and 50−60 steel balls (4.5-mm diameter) were added. The flask was gently agitated for 30 min and over this period the solid became slightly damp. Sublimation at 80 °C under vacuum afforded a white product. Yield: 0.16 g (19%). mp = 120 °C (dec). Anal. Calcd for B₆H₁₆-Mg: H, 15.3; B, 61.6; Mg, 23.1. Found: H, 15.0; B, 60.2; Mg, 23.1. IR (cm⁻¹): 2543 vs, 2479 vs, 2316 vs, 2175 w, 1298 sh, 1134 vs, 1043 w, 981 vs, 829 s.

**Bis(octahydrotriborato)bis(diethylether)magnesium, Mg-(B₃H₈)₂(Et₂O)₂, (2).** Solid MgBr₂(Et₂O) (4.0 g, 15.5 mmol) and NaB₃H₈ (1.0 g, 15.8 mmol) were ground together briefly in a mortar and pestle. The mixture was transferred a 250 mL round-bottomed flask, and 50−60 steel balls (4.5-mm diameter) were added. The flask was gently agitated for 30 min and over this period the solid became slightly damp. Sublimation at 70 °C under vacuum afforded white crystals. Yield: 0.82 g (41%). mp = 40 °C. Anal. Calcd for C₄H₃₆B₆O₂Mg: C, 37.9; H, 14.3; B, 25.6; Mg, 9.59. Found: C,

37.5; H, 14.1; B, 25.6; Mg, 9.71. MS(FI) [fragment ion, relative abundance]: $m/z = 139$ [Mg(B$_3$H$_8$)(Et$_2$O)$^+$, 20], 213 [Mg(B$_3$H$_8$)-(Et$_2$O)$_2$$^+$, 25], 302 [Mg$_2$(B$_3$H$_8$)(B$_5$H$_{12}$)(Et$_2$O)$^+$, 20], 318 [Mg$_2$-(B$_3$H$_8$)$_3$(Et$_2$O)$_2$$^+$, 100]. $^1$H NMR (O(C$_2$D$_5$)$_2$, 20 °C): $\delta$ 3.77 (q, $^3J_{HH}$ = 8 Hz, 8H, CH$_2$), 1.50 (t, $^3J_{HH}$ = 8 Hz, 12H, CH$_3$), 0.52 (br, fwhm = 125 Hz, 16H, B$_3$H$_8$). IR (cm$^{-1}$): 2506 vs, 2448 vs, 2302 vs, 2129 m, 1289 w, 1262 w, 1189 w, 1148 s, 1092 s, 1034 s, 992 s, 891 m, 865 w, 832 m, 778 s, 692 w.

**Magnesium Dibromide·1.5Dimethylether, MgBr$_2$(Me$_2$O)$_{1.5}$.** Solid MgBr$_2$ (6.3 g, 34 mmol) was cooled to $-78$ °C and Me$_2$O (50 mL) was condensed onto the solid. After the mixture had been stirred for 4 h, the Me$_2$O was removed under vacuum to afford a white solid. Yield: 8.84 g (98%). Anal. Calcd for C$_3$H$_9$O$_{1.5}$Br$_2$-Mg: C, 14.2; H, 3.58. Found: C, 14.0; H, 3.42.

**Bis(octahydrotriborato)bis(dimethylether)magnesium, Mg-(B$_3$H$_8$)$_2$(Me$_2$O)$_2$, (3).** Solid MgBr$_2$(Me$_2$O)$_{1.5}$ (1.86 g, 7.35 mmol) and NaB$_3$H$_8$ (1.09 g, 17.2 mmol) were ground together briefly in a mortar and pestle. The mixture was transferred to a 100 mL round-bottomed flask, and 30–40 steel balls (4.5-mm diameter) were added. The flask was gently agitated for 15 min and over this period the solid became slightly damp. Sublimation at 75 °C under vacuum afforded white crystals. Yield: 0.25 g (25%). mp = 55 °C. Anal. Calcd for C$_2$H$_{28}$B$_6$O$_2$Mg: C, 24.3; H, 14.3; B, 32.9; Mg, 12.3. Found: C, 23.9; H, 14.0; B, 33.1; Mg, 13.0. MS(FI) [fragment ion, relative abundance]: $m/z = 111$ [Mg(B$_3$H$_8$)(Me$_2$O)$^+$, 40], [Mg-(B$_3$H$_8$)(Me$_2$O)$_2$$^+$, 45], 216 [Mg$_2$(B$_3$H$_8$)$_3$(Me$_2$O)$^+$, 20], 262 [Mg$_2$-(B$_3$H$_8$)$_3$(Me$_2$O)$_2$$^+$, 100], 276 [Mg$_2$(B$_3$H$_8$)$_3$(BH$_4$)(Me$_2$O)$_2$$^+$, 15], 308 [Mg$_2$(B$_3$H$_8$)$_3$(Me$_2$O)$_3$$^+$, 10]. IR (cm$^{-1}$): 2493 vs, 2449 vs, 2301 vs, 2129 s, 1260 s, 1154 s, 1048 s, 973 w, 893 s, 812 m, 757 w.

**Bis(cyclopentadienyl)(tetrahydrofuran)magnesium, Cp$_2$Mg-(thf), (4).** A mixture of [CpMgCl(Et$_2$O)]$_2$[37] (1.46 g, 3.9 mmol) and NaB$_3$H$_8$ (0.50 g, 7.9 mmol) was placed in a 100 mL round-bottom flask equipped with ~40 glass beads (3-mm diameter) and a magnetic stirring bar. Degassed pentane (50 mL) was added, and the mixture was stirred vigorously at room temperature. After 8 h, thf (1.3 mL, 8.0 mM) was added and the mixture was stirred overnight. The white precipitate was collected by filtration and dried under vacuum. Sublimation under vacuum at 90 °C afforded white crystals. Yield: 0.32 g (18%). Anal. Calcd for C$_{14}$H$_{18}$OMg: C, 74.2; H, 8.01. Found: C, 74.4; H, 7.63.

**CVD from Mg(B$_3$H$_8$)$_2$(Et$_2$O)$_2$ and Mg(B$_3$H$_8$)$_2$(Me$_2$O)$_2$.** Deposition of thin films was carried out in an ultrahigh vacuum (UHV) chamber equipped with a turbomolecular pump having a base pressure of $5 \times 10^{-9}$ Torr; details of the construction of the chamber have been published elswhere[23] For both precursors **2** and **3**, the stainless steel precursor reservoir was heated to 70 °C to increase the precursor transport rate. Precursors were delivered to the Si-(100) surface by means of an argon carrier gas (10 sccm) flowing through 0.25 in. (6.35 mm) o.d. stainless steel tubes. The silicon substrates were degreased by successive sonications in tetrachloroethylene, acetone, isopropanol, and deionized water for 10 min each. To remove the native oxide on the surface, the degreased silicon substrates were immersed in a 10% HF solution and then rinsed with deionized water. Silicon substrates were heated by passing an electric current through the substrate, and the surface temperature was determined by means of an infrared pyrometer.

**Crystallographic Studies.**[38] Single crystals of all three compounds, grown by sublimation, were mounted on glass fibers with Krytox oil (DuPont) and immediately cooled to $-80$ °C in a cold nitrogen gas stream on the diffractometer. Data were collected with an area detector by using the measurement parameters listed in Table 1. The measured intensities were reduced to structure factor amplitudes and their estimated standard deviations by correction for background and Lorentz and polarization effects. Systematically absent reflections were deleted and symmetry-equivalent reflections were averaged to yield the sets of unique data. The analytical approximations to the scattering factors were used, and all structure factors were corrected for both real and imaginary components of anomalous dispersion. All structures were solved using direct methods (SHELXTL). The correct positions for all non-hydrogen atoms were deduced from E-maps. Final refinement parameters are given in Table 1. A final analysis of variance between observed and calculated structure factors showed no apparent errors. Subsequent discussions for compounds **2–4** will be divided into individual paragraphs.

**(a) 2.** Although the orthorhombic lattice and systematic absences suggested the space group to be $P222_1$, the actual space group is $P2_12_12$ with the second screw axis exhibiting weak violations of the systematic absences, probably owing to Renninger effects. All 1750 unique reflections were used in the least-squares refinement. Although corrections for crystal decay were unnecessary, a face-indexed absorption correction was applied. The quantity minimized by the least-squares program was $\sum w(F_o^2 - F_c^2)^2$, where $w = \{[\sigma(F_o^2)]^2 + 1.22P\}^{-1}$ and $P = (F_o^2 + 2F_c^2)/3$. Hydrogen atoms were located in the difference maps, and their positions were refined with independent isotropic displacement parameters. Chemically similar B–H and C–H distances were constrained to equal within 0.01 Å. An isotropic extinction parameter was refined to a final value of $x = 1.37(5) \times 10^{-5}$ where $F_c$ is multiplied by the factor $k[1 + F_c^2 x \lambda^3 / \sin 2\theta]^{-1/4}$ with $k$ being the overall scale factor. Successful convergence was indicated by the maximum shift/error of 0.000 for the last cycle. The largest peak in the final Fourier difference map (0.20 e·Å$^{-3}$) was located 1.25 Å from H13.

**(b) 3.** Systematic absences for $0kl$ ($k + l \neq 2n$) and $h0l$ ($l \neq 2n$) were consistent with space groups $Pca2_1$ and $Pbcm$; the non-centrosymmetric $Pca2_1$ was shown to be the correct choice by successful refinement of the proposed model. All 2837 unique reflections were used in the least-squares refinement. Although corrections for crystal decay were unnecessary, a face-indexed absorption correction was applied. The quantity minimized by the least-squares program was $\sum w(F_o^2 - F_c^2)^2$, where $w = \{[\sigma(F_o^2)]^2 + (0.0386P)^2\}^{-1}$ and $P = (F_o^2 + 2F_c^2)/3$. Boron-bound hydrogen atoms were located in the difference maps and refined without constraints; these hydrogen atoms were each given independent isotropic displacement parameters. Methyl hydrogen atoms were placed in idealized tetrahedral locations with C–H = 0.98 Å and optimized by rotation about C–O bonds; their displacement parameters were set equal to $1.5U_{eq}$ for the attached carbon. No correction for isotropic extinction was necessary. Successful convergence was indicated by the maximum shift/error of 0.000 for the last cycle. The largest peak in the final Fourier difference map (0.09 e·Å$^{-3}$) was located 0.87 Å from O1.

**(c) 4.** Systematic absences for $hkl$ ($h + k \neq 2n$) and $h0l$ ($l \neq 2n$) were consistent with space groups $Cc$ and $C2/c$; the last of these was suggested by the average values of the normalized structure factors and proven to be the correct choice by the success of the subsequent refinement. All 1161 unique reflections were used in the least-squares refinement. Although corrections for crystal decay were unnecessary, a face-indexed absorption correction was applied.

(37) Prepared from Mg(i-Pr)Cl and CpH in Et$_2$O; see also Dohmeier, C.; Loos, D.; Robl, C.; Schnöckel, H.; Fenske, D. *J. Organomet. Chem.* **1993**, *448*, 5–8.

(38) For details of the crystallographic methods used see: Brumaghim, J. L.; Priepot, J. G.; Girolami, G. S. *Organometallics* **1999**, *18*, 2139–2144.

The quantity minimized by the least-squares program was $\sum w(F_o^2 - F_c^2)^2$, where $w = \{[\sigma(F_o^2)]^2 + (0.053P)^2\}^{-1}$ and $P = (F_o^2 + 2F_c^2)/3$. Hydrogen atoms were located in the difference maps, and their positions were refined subject to the constraint that chemically similar C−H bond distances were equal within 0.01 Å; their displacement parameters were set equal to $1.2U_{eq}$ for the attached carbon. Successful convergence was indicated by the maximum shift/error of 0.001 for the last cycle. The largest peak in the final Fourier difference map (0.41 e·Å$^{-3}$) was located 1.13 Å from O1.

**Supporting Information Available:** Crystallographic data in cif format. This material is available free of charge via the Internet at http://pubs.acs.org.

**Note Added in Proof.** The use of $Mg(BH_4)_2$ as a CVD precursor has recently been described. The films obtained at 500 °C are amorphous, boron-rich ($MgB_x$ with $x > 6$), and contain significant amounts of surface oxygen. Crociani, L.; Rossetto, G.; Kaciulis, S.; Mezzi, A.; El-Habra, N.; Palmieri, V. *Chem. Vap. Depos.* **2007**, *13*, 414−419.

IC701037T